ISSN: 2977-0041

Research Article

Journal of Material Sciences and Engineering Technology

Tuning Dielectric and Electrical Properties of Barium Calcium Titanate via Gd and Fe Co-Doping

Poonam Deswal, Anshu Gaur and Ahamad Mohiddon MD*

Center for Nanoscience and Nanotechnology, Department of Physics, Faculty of Science and Humanities, SRM University Delhi-NCR, Sonepat 131029, Haryana, India

***Corresponding author**
Ahamad Mohiddon MD, Center for Nanoscience and Nanotechnology, Department of Physics, Faculty of Science and Humanities, SRM University Delhi-NCR, Sonepat 131029, Haryana, India.

Received: July 15, 2025; **Accepted:** July 25, 2025; **Published:** August 07, 2025

ABSTRACT

In the present work, the dielectric and electrical properties of 6% Gd and Fe co-doped Barium Calcium Titanate (BCT) ceramics are investigated. $Ba_{0.9}Ca_{0.1}Ti_{1-x}(Gd_{0.5}Fe_{0.5})_xO_3$ (BCTGF) was synthesized by the sol-gel method with calcination at 1000°C and the compressed pellet's sintering at 1350°C. Gd, Fe co-doped BCT was found in a single phase with a tetragonal crystal structure as confirmed from the X-ray diffraction data analysis. The ferroelectric to paraelectric transition temperature of the composition is at 54°C, lower than that of pure BCT. The dynamic aspect of the dipoles is analyzed using frequency-dependent dielectric response.

Keywords: Electrical, Barium Calcium Titanate, Crystallographic Investigation

Introduction

The growing need for high-performance, sustainable, and efficient energy systems to power electric cars, portable gadgets, and renewable energy grids has made energy storage a crucial area of focus in contemporary technology. Good energy storage materials need to be thermally stable to continue to function under a variety of operating conditions, they must have a high dielectric permittivity to store a sizable amount of electric energy per unit volume, and have an exceptional electrical breakdown strength to guarantee sustainability at high voltages. Ferroelectric ceramics, like barium titanate (BT), barium strontium titanate (BST), and barium calcium titanate (BCT), are among the most promising materials for energy storage because of their effective electrical energy storage and release capabilities. BT is a well-known perovskite ceramic that serves as a parent compound for a wide range of lead-free ferroelectric and dielectric materials. Due to its excellent dielectric constant, strong ferroelectric behavior and thermal stability, BT forms the base structure for many solid solution systems. By substituting elements at the A-site (Ba^{2+}) or B-site (Ti^{4+}) such as in Barium Calcium Titanate (BCT) or Barium Strontium Titanate (BST), its physical properties can be tailored to enhance performance in capacitors, sensors and energy storage devices. BT's versatility and environmental friendliness make it an ideal parent material for developing next-generation green electronic materials. Among the modified BT compositions, Barium Calcium Titanate ($Ba_{1-x}Ca_xTiO_3$-BCT) is a promising candidate with its ferroelectric to paraelectric phase transition falling in the range of room temperature to 120°C based on Ca concentration in BCT. BCT ceramics have demonstrated good electrical breakdown strength and strong thermal stability, which supports reliable energy storage at high voltages and efficient operation across a wide temperature range respecctively. However, Ca doping deteriorates the ferroelectric properties of BCT. Therefore, a constant effort is being carried out for reducing phase transition temperature near to room temperature without losing its ferroelectric characteristics, by modifying with various dopants. It is expected that the combined presence of both Gd and Fe in BCT ceramics can lead a significant increase in the dielectric constant due to the enhanced

Citation: Poonam Deswal, Anshu Gaur, Ahamad Mohiddon MD. Tuning Dielectric and Electrical Properties of Barium Calcium Titanate via Gd and Fe Co-Doping. J Mat Sci Eng Technol. 2025. 3(3): 1-5. DOI: doi.org/10.61440/JMSET.2025.v3.64

polarization effects. In the present work, the effect of 6% Gd and Fe co-doping on electrical and dielectric properties of Barium Calcium Titanate (BCT) ceramics is investigated [1,2].

Experimentation

$Ba_{0.9}Ca_{0.1}Ti_{1-x}(Gd_{0.5}Fe_{0.5})_xO_3$ (BCTGF) was synthesized by sol-gel method. The constituent materials used for synthesis are Barium acetate (ACS, 99-102%) $Ba(OOCCH_3)_2$, Calcium nitrate tetrahydrate (98%) $Ca(NO_3).4H_2O$, Gadolinium Nitrate (99.9%) $Gd(NO_3)_3.6H_2O$, Iron nitrate nonahydrate (ACS, 98-100%) $Fe(NO_3)_3.9H_2O$, Titanium tetra-isopropoxide (97%) $C_{12}H_{28}O_4Ti$. A 40 mL citric acid solution of 2 M was prepared in distilled water. This solution was divided into two parts. In one part (20 mL) titanium tetra-isopropoxide was dissolved on a magnetic stirrer (for 3 h) until it dissolved completely and becomes a transparent solution. In another part of the solution, Barium acetate is dissolved followed by calcium nitrate, gadolinium nitrate and iron nitrate nonahydrate sequentially. These A-site and B-site cation solutions were mixed and stirred for 30 min, which resulted in the formation of a viscous solution. Ethylene glycol ($C_2H_6O_2$) was added to the mixture and stirred for around 30 min. Finally, ammonia solution was added, which turns the mixture into a transparent gel. The obtained gel was dried in hot air oven for 24 h and ground to a fine powder in a mortar. The fine powder was calcined at 1000°C for 12 h in a muffle furnace. The crystalline structure of the calcined powder was identified by X-ray diffraction technique (XRD). The XRD patterns were recorded at room temperature using an X-ray diffractometer (PANalytical X'pert Pro) with Cu-Kα radiation (λ = 1.5406 Å). Data were collected over a 2θ range of 20° to 70° with a step size of 0.0167°. The calcined powder was densified into pellets by applying 1 GPa pressure beneath the uniaxial pelletizer [2]. These compacted pellets were sintered at 1350°C for 2 h. For the dielectric measurements, the pellets were polished and coated with silver paste on both sides, followed by curing at 200 °C to ensure good electrical contact. The temperature dependence of the dielectric characterisation of BCTGF sintered pellets was carried out in the range of 30°C to 300°C at the four discrete frequencies, 200Hz, 2kHz, 20kHz, 200kHz using impedance analyser (Model-ZN2376, nF corporation, Japan) equipped with high temperature furnace RT-1000°C (Wayne kerr electronics, India). Dielectric characteristics were also measured as a function of frequency from 20 Hz to 2 MHz at various temperatures starting from 50°C to 500°C in steps of 50°C.

Results and Discussion

Crystallographic Investigation

The X-ray diffraction analysis was carried out to investigate the phase composition and crystallographic structure of the synthesized $Ba_{0.9}Ca_{0.1}Ti0.94(Gd_{0.5}Fe_{0.5})0.06O_3$ (BCTGF) composition and is presented in the Figure 1. The XRD patterns confirm the formation of a single-phase perovskite structure with no detectable secondary phases, indicating the successful incorporation of Gd^{3+} and Fe^{3+} ions into the BCT lattice. All the diffraction peaks are indexed to a tetragonal phase (space group P4mm), similar to the undoped BCT system, with the help of JCPDS file no. 05-0626. Rietveld refinement was carried out by the FullProf suite software and the refined data, along with the residual data, are included in Figure 1. The lattice parameters extracted from the refined data are a = b = 3.9711 Å, c =3.9961 Å, with a degree of tetragonality represented by c/a ratio as 1.0062. This data agrees with the literature (a = b = 3.9593 Å, c = 3.9995 Å) 4. A slight expansion of the unit cell is observed, attributed to the substitution by larger Gd^{3+} and Fe^{3+} ions ($r^{3+}_{6(Gd)}$ = 0.938Å and $r^{3+}_{6(Fe)}$ = 0.645 Å, respectively) at the Ti^{+4} (r^{4+}_6 = 0.605 Å) sites. These XRD observations indicate the successful incorporation of dopants into the BCT perovskite lattice.

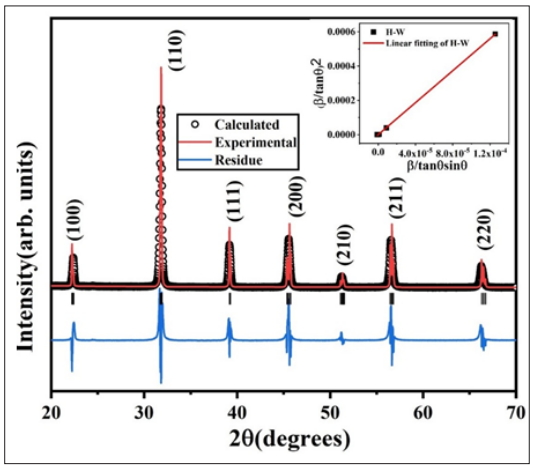

Figure 1: The experimental and Rietveld refined XRD data of the $Ba_{0.9}Ca_{0.1}Ti_{0.94}(Gd_{0.5}Fe_{0.5})_{0.06}O_3$ calcined at 1000°C for 12 h along with the Haldar-Wagner plot for determining average crystalline size and strain, shown in the inset

The structural stability of the synthesized perovskite compound $Ba_{0.9}Ca_{0.1}Ti_{0.94}(Gd_{0.5}Fe_{0.5})_{0.06}O_3$ was assessed by calculating the Goldschmidt tolerance factor (t), which provides insight into the degree of distortion from the ideal cubic perovskite lattice. The tolerance factor was determined using the ionic radii of the A-site, B-site and the O-site ions of the ABO_3 type structure

$$Tolerance\ factor\ (t) = \frac{r_A + r_O}{\sqrt{2}(r_B + r_O)} \quad (1)$$

where r_A , r_B and r_O are the ionic radii of A-site, B-site and the O-site ions. The calculated value of the tolerance factor for Gd and Fe co-doped BCT composite is 1.04 which is smaller than that for pure BCT (1.05). The value of t close 1 indicates the stable perovskite structure and t = 1 represents cubic perovskite structure eg. $SrTiO_3$. A deviation of t from t =1 is the signature of asymmetry introduced in the unit cell. Our analysis indicates a tetragonal crystal structure of the BCTGF. Further, the refined XRD data was utilised to extract the crystallite size information of the BCTGF composition using the Debye–Scherer formula, given as,

$$D = \frac{k\lambda}{\beta_{1/2}\cos\theta} \quad (2)$$

where D is the crystallite size, k is the shape factor (0.89), λ is the wavelength of X-rays (1.5406 Å), $\beta_{1/2}$ is the full width at half maximum (FWHM) of the most intense peak, and θ is the Bragg angle. The crystallite size calculation was carried out using the strongest XRD peak centred at 2θ = 31.804 °, i.e. (110) peak. D is observed to be 27.8 nm, which indicates the nanocrystalline nature of the sample. In an alternate technique, the crystallite size D and lattice strain ε of the sample were estimated using the Haldar–Wagner (H–W) method. The H–W method incorporates a Gaussian distribution model to account for inhomogeneous lattice

strain, making it more suitable for complex or doped perovskite systems. The relationship between the FWHM (β) of XRD peaks with crystallite size (D) and the lattice strain (ε) is given by,

$$\left(\frac{\beta}{\tan\theta}\right)^2 = \frac{k\lambda\beta}{D\tan\theta\sin\theta} + 16\varepsilon^2 \quad (3)$$

with θ as the Bragg angle, λ the X-ray wavelength (= 1.5406 Å). This is the equation of a straight line with x-axis as the $\beta/(\sin\theta.\tan\theta)$ and y-axis as the $(\beta/\tan\theta)2$ with kλ/D as slope and $16\varepsilon^2$ as intercept. The graphs plotted according to equation (3) and fitted linearly are shown in the inset of Figure 1. The average crystalline size D = 29 nm and the strain ε = 1.197 × 10^{-4} are extracted from slope and intercept. The positive lattice strain indicates the tensile nature of the strain developed in the lattice. These microstructural changes are expected to play a significant role in modulating the dielectric and ferroelectric behavior of the ceramics. The theoratical density of Gd and Fe co-doped BCT was calculated by the relation $\rho = \frac{nM}{N_a V}$, where M is molecular weight, N_a is the Avogadro's number, n is the number of molecules per unit cell, V (= ac^2) is the volume of the unit cell, a and c are unit cell parameters of tetragonal unit cell, obtained from the XRD data analysis. The density of the compound is 5.86 g/cm^3. From the dimensions of the sintered pellets and its mass, the density of the BCTGF pellet is calculated and is observed to be 5.07 g/cm^3.

Overall, these results confirm that Gd and Fe co-doping does not disrupt the perovskite structure but subtly modifies the lattice, which is expected to influence the dielectric and electrical properties of the BCTGF ceramics.

Dielectric Performance Analysis

The temperature dependence of the dielectric constant (ε′) and dielectric loss (tan δ) of BCTGF sintered pellets measured in the range of 30°C to 300°C at the four discrete frequencies 200Hz, 2kHz, 20kHz, 200kHz are presented in Figure 2(a) and 2(b) respectively. The dielectric constant in Figure 2(a) exhibited a prominent dielectric anomaly, with ε′ increasing gradually with temperature and reaching a maximum at a specific transition temperature (T_m = 54°C), which is associated with the ferroelectric–paraelectric phase transition. The incorporation of Gd^{3+} and Fe^{3+} ions in the B-site brought down the phase transition temperature towards the room temperature from 120°C of pure BCT[5].

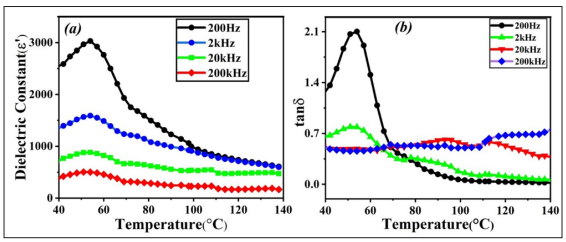

Figure 2: Variation of (a) dielectric constant and (b) dielectric loss as a function of temperature measured at different frequencies of $Ba_{0.9}Ca_{0.1}Ti_{0.94}(Gd_{0.5}Fe_{0.5})_{0.06}O_3$.

The sharpness of the peak diminished with Gd^{3+}/Fe^{3+} doping. This behaviour can be attributed to compositional disorder at the B-site, which introduces local structural distortions and impedes long-range ferroelectric ordering. At temperatures above T_m, ε′ decreases steadily, as expected for the paraelectric phase. The temperature dependence of the dielectric constant (ε′) of BCTGF pellet was analysed to determine the ferroelectric–paraelectric phase transition characteristics as presented in Figure 3(a). In the paraelectric region ($T > T_c$), the inverse dielectric constant (1/ε′) follows the Curie–Weiss law:

$$\varepsilon' = \frac{C}{T - T_C} \quad (4)$$

where ε′ is the dielectric constant, T is the absolute temperature, T_c is the Curie temperature, and C is the Curie–Weiss constant. A linear fit of the 1/ε′ versus T plot above the transition temperature confirms the applicability of the Curie–Weiss law. The values of Tc and C are calculated from the linear fit of the data in the paraelectric region of 330K to 370K and are tabulated in Table 1 for different measured frequencies. The value of C extracted from the above fit is in agreement with the values that are reported for typical perovskite ferroelectric materials like BCT, BST 6, and BNST 7. From Table 1, it is evident that the C value decreases with measured frequency from 2 kHz to 200 kHz, which is a typical characteristic of ferroelectric materials. At higher frequencies, the electric dipoles are unable to follow the oscillations of the applied electric field. This is the same reason for decreasing the maximum dielectric constant at T_m with increasing frequency. Further, the T_c is observed to shift with applied frequency, which is a typical nature of relaxor ferroelectrics. However, no systematic trend is recorded with increasing frequency. The change in the Tc at different frequencies may be attributed to the local heterogeneities developed due to the doping of Gd^{3+} and Fe^{3+} in BCT.

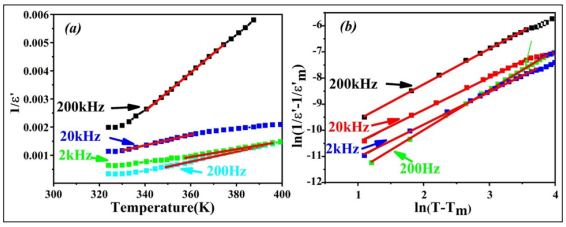

Figure 3: (a) Curie-Weiss law plot for determining the Curie temperature and Curie-Weiss Constant (b) modified Curie-Weiss law plot for determining diffusion coefficients of $Ba_{0.9}Ca_{0.1}Ti_{0.94}(Gd_{0.5}Fe_{0.5})_{0.06}O_3$ sample.

To further investigate the nature of the phase transition in BCTGF pellets, the temperature dependence of the dielectric constant was evaluated using the modified Curie –Weiss law

$$\frac{1}{\varepsilon'} - \frac{1}{\varepsilon'_m} = \frac{(T - T_m)^\gamma}{2\varepsilon'_m\delta^2} \quad (5)$$

where ϵ′ is the dielectric constant at absolute temperature (T), ϵ′m is the maximum value of dielectric constant at the transition temperature Tm, which is correlated to the C parameter of Curie Weiss law (equation 4), and γ, δ are the diffuseness coefficients. The values of γ and δ was obtained from the slope and intercept of the linear fit of the plot ln (1/ ϵ′-1/ ϵ'_m) versus ln(T-T_m) presented in Figure 3(b). The values of both coefficients are included in Table 1 for the four discrete measured frequencies. The resulting γ values ranging between 1.24 and 1.52 indicate partially diffuse phase transition behaviour of BCTGF.

Table 1: Curie-Weiss law and modified Curie-Weiss law extracted parameters of $Ba_{0.9}Ca_{0.1}Ti_{0.94}(Gd_{0.5}Fe_{0.5})_{0.06}O_3$.

Frequency (Hz)	TC (K)	C (K)	ε_m'	δ	γ	E_a at high T (eV)	E_a at low T (eV)
200	316	0.5647×105	3029.16	8.76	1.52	0.73	0.87
2k	292	0.7264×105	1590.17	8.23	1.24	0.63	0.94
20k	267	0.538×105	881.91	8.28	1.24	0.67	0.78
200k	303	0.145×105	502.53	7.54	1.35	0.50	0.45

The a.c conductivity (σ_{ac}) behaviour of BCTGF sample was investigated over a frequency range of 200 Hz to 200 kHz and in the temperature range of 30ºC to 500ºC. The frequency-dependent *a.c* conductivity (σ_{ac}) was calculated using the relation

$$\sigma_{ac} = \omega\epsilon_0 \epsilon''(\omega) \quad (6)$$

where $\omega = 2\pi f$ is the angular frequency, ϵ_0 is vacuum permittivity and $\epsilon''(\omega)$ is the imaginary part of the complex dielectric constant. At lower frequencies, σ_{ac} remains nearly constant. As the frequency increases, σ_{ac} increases gradually which is attributed to the enhanced hopping of charge carriers between localized states. With increasing temperature, σ_{ac} increases across all frequency regions, indicating the semiconducting nature of the material. The rise in conductivity with temperature is due to the increased thermal energy, which enhances the mobility of charge carriers and facilitates their hopping over potential barriers. The substitution of Ti^{+4} with Gd^{3+} and Fe^{3+} introduces defect states and oxygen vacancies, which further contribute to carrier concentration and reduce the activation energy for conduction. For calculating the activation energy required to produce the conduction mechanism, an equation known as the Arrhenius equation is considered. The conductivity variation with temperature according to the Arrhenius relation is given as,

$$\sigma_{ac} = \sigma_0 \exp\left(\frac{-E_a}{KT}\right) \quad (7)$$

Where σ_0 is a pre-exponential factor, E_a is the activation energy, K is the Boltzmann constant, and T is the absolute temperature. A graph between ln σ_{ac} and $10^3/T$ shows a linear behaviour (Figure 4). The Slope of this linear portion obtained from the linear fitting provides the value of activation energy (E_a). The value of activation energy (E_a) for the four discrete frequencies at high and low temperatures shown in Table 1.

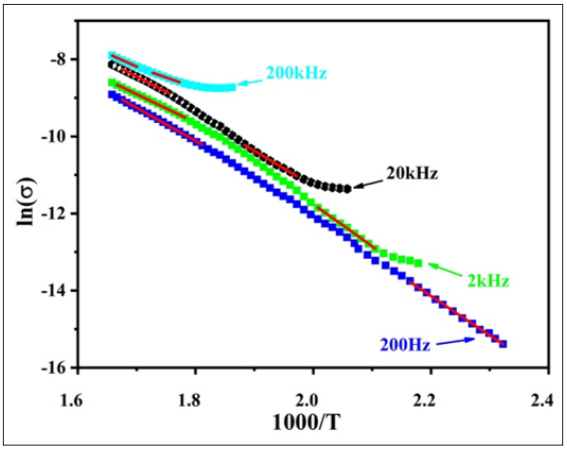

Figure 4: Linear fitting graph for the variation of ln(σ) with 1/T for finding activation energy

The Figure 5 (a and b) illustrates the frequency dependence of the real (ε') and imaginary ε' and ε'' parts of the dielectric permittivity of BCTGF as a function of frequency at various temperatures (300–500°C) are shown in Figure 5. Both ε' and ε'' decrease sharply with increasing frequency, a typical behaviour for perovskite ceramics, indicating strong dielectric dispersion at low frequencies due to interfacial polarization and space charge effects. As temperature increases, both ε' and ε'' values rise significantly, especially at lower frequencies, suggesting enhanced mobility of charge carriers and increased polarization with thermal activation. The co-doping of BCT with Gd and Fe ions introduces additional oxygen vacancies and defect dipoles, which enhance space charge polarization and contribute to the observed increase in dielectric permittivity. Gd^{3+} and Fe^{3+} ions, substituting the A and B sites of the perovskite lattice, respectively, disrupt the long-range ferroelectric order and facilitate hopping conduction, further amplifying dielectric losses (as seen in the rise of ε''). This behaviour is consistent with previous studies, where rare-earth and transition metal doping in $BaTiO_3$-based ceramics resulted in increased dielectric constant and loss due to defect-induced polarization mechanisms [8,9]. The dielectric relaxation behaviour of the BCTGF sample was investigated using the Cole-Cole model, which provides a generalized framework to describe dispersion in materials exhibiting non-ideal, broad relaxation processes.

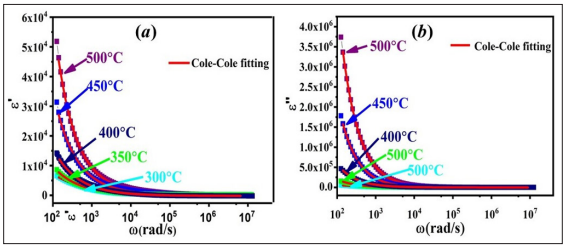

Figure 5: Variation of (a) real part and (b) imaginary part of dielectric permittivity for $Ba_{0.9}Ca_{0.1}Ti_{0.94}(Gd_{0.5}Fe_{0.5})_{0.06}O_3$ at different temperatures along with Cole-Cole fitting.

The variation of complex dielectric permittivity ε*(ω) as a function of angular frequency ω, is expressed by the Cole-Cole relation, given as,

$$\epsilon^* = \epsilon_\infty + \frac{\epsilon_S - \epsilon_\infty}{1 + (i\omega\tau)^{1-\alpha}} \quad (8)$$

$$\epsilon''(\omega) = \frac{(\epsilon_S - \epsilon_\infty)}{2}\left(1 - \frac{\sin(1-\alpha)x}{\cosh(1-\alpha)x - \cos\alpha\pi/2}\right) \quad (9)$$

$$\epsilon''(\omega) = \frac{(\epsilon_S - \epsilon_\infty)}{2}\left(\frac{\sin(1-\alpha)x}{\cos(1-\alpha)x - \cos\alpha\pi/2}\right) \quad (10)$$

In this expression, ϵ‘ and ϵ" denote the real and imaginary parts of the complex permittivity, respectively; ϵ_s is the static dielectric constant; ϵ_∞ is the high-frequency limit of the permittivity; τ is the characteristic relaxation time and α is the Cole-Cole parameter such that $0 \leq \alpha < 1$, and quantifies the symmetric broadening of the relaxation peak. The Cole–Cole model is used to describe dielectric relaxation with a distribution of relaxation times, characterized by the α-value (distribution parameter). In Figure 5, the Cole–Cole fitting curve shown by the red lines closely matches the experimental data. Table 2 provides the values of α and τ obtained from modelling ε′(ω) and ε″(ω) using Eq. 9 and 10. The observed α values (ranging from 0.25 to 0.39 for ε′ and 0.0163 to 0.049 for ε″) confirm a significant non-Debye character, which is typical for co-doped perovskite ceramics. The difference between α obtained from ε′(ω) and ε″(ω) indicates the presence of DC conduction in the system. It is noted that both parameters vary with temperature, reflecting changes in the relaxation dynamics of the system.

Table 2: Cole-Cole relation extracted parameter of $Ba_{0.9}Ca_{0.1}Ti_{0.94}(Gd_{0.5}Fe_{0.5})_{0.06}O_3$.

Temperature (˚C)	Real Part (ϵ‘)		Imaginary Part (ϵ")	
	α	τ (s)	α	T
300	0.29	0.0065	0.016	0.01346
350	0.39	0.4384	0.049	0.0681
400	0.30	0.1978	0.040	0.0604
450	0.29	0.104	0.002	0.04187
500	0.25	0.0865	0.030	0.117

As temperature increases, the mobility of charge carriers and the contribution of space charge polarization also increase, leading to higher values of ϵ′ and ϵ″, as observed in the Figure 5. The non-zero values of α indicate a broad distribution of relaxation times, typical for materials with significant structural disorder and defect-induced polarization, as introduced by Gd^{3+} and Fe^{3+} doping. The increase in τ with temperature for the imaginary part suggests that the relaxation process becomes slower, likely due to enhanced interaction among defect dipoles and increased conductivity at higher temperatures. The τ values represent the characteristic relaxation times, which generally decrease with temperature, reflecting the thermally activated nature of the relaxation process [8,9].

Conclusion

$Ba_{0.9}Ca_{0.1}Ti_{0.94}(Gd_{0.5}Fe_{0.5})_{0.06}O_3$ ceramics were successfully synthesized in a single phase using sol-gel method. XRD data analysis by the Rietveld refinement method suggested the tetragonal crystal structure, with the lattice distortion due to the incorporation of Gd^{3+} and Fe^{3+} ions. The average crystallite size of Fe and Gd co-modified BCT calculated via Debye-Scherrer method is 27.8 nm, which closely resembles the results obtained using the Haldar-Wagner method i.e. 29 nm. The substitution of Gd^{3+} and Fe^{3+} at the Ti4+ site led to improved polarization and dielectric constant, which is associated with introduced defect dipoles and modified grain boundary dynamics. Furthermore, reduced dielectric loss makes the BCTGF ceramics promising candidates for capacitor and memory device applications. These findings demonstrate that targeted co-doping in $Ba_{0.9}Ca_{0.1}TiO_3$-based ceramics is an effective strategy for tuning multifunctional properties.

Acknowledgements

The authors acknowledge Prof. S. Srinath and the School of Physics, University of Hyderabad, for providing the XRD characterization facility.

References

1. Correia T, Zhang Q. Electrocaloric effect: an introduction. InElectrocaloric Materials: New Generation of Coolers. Berlin, Heidelberg: Springer Berlin Heidelberg. 2013. 29: 1-15.
2. Puli VS, Pradhan DK., Riggs BC, Chrisey DB, Katiyar RS. Investigations on structure, ferroelectric, piezoelectric and energy storage properties of barium calcium titanate (BCT) ceramics. J Alloys Compd. 2014. 584: 369-373.
3. Ji X, Wang C, Li S, Zhang S, Tu R, et al. Structural and electrical properties of BCZT ceramics synthesized by sol–gel process. Journal of Materials Science: Materials in Electronics. 2018. 29: 7592-7599.
4. Merselmiz S, Hanani Z, Ben Moumen S, Matavž A, Mezzane D, et al. Enhanced electrical properties and large electrocaloric effect in lead-free Ba0. 8Ca0. 2Zr x Ti1− x O3 (x= 0 and 0.02) ceramics. Journal of Materials Science: Materials in Electronics. 2020. 31: 17018-17028.
5. Li LY, Tang XG. Effect of electric field on the dielectric properties and ferroelectric phase transition of sol-gel derived (Ba0.90Ca0.10)TiO3 ceramics. Mater Chem Phys. 2009. 115: 507-511.
6. Saroha P, Mohiddon, Md, Preeti A, Gaur A. Impedance spectroscopy investigation and structural characterization of yttrium and lithium modified Barium Strontium Titanate composite. Mater Today Proc. 2023.
7. Kumar A, Kumar R, Singh K, Singh S. Enhanced Electrocaloric Effect and Energy Storage Density in Lead-Free 0.8Na 0.5 Bi 0.5 TiO 3 -0.2SrTiO 3 Ceramics. Physica Status Solidi (A) Applications and Materials Science. 2019. 216.
8. Kumar R. Enhanced dielectric and electrical properties of Gd and Fe co-Adoped $BaTiO_3$ ceramics. Ceramics International. 2021.
9. Zhang J. Effect of rare-earth and transition metal co-doping on the dielectric properties of $BaTiO_3$ ceramics.Journal of Alloys and Compounds. 2020.